Distributed cooperative control framework of a cryogenic system

Haiyang Ding, Mazen Alamir, Francois Bonne, Ahmad Hably, Patrick Bonnay

Distributed cooperative control framework of a cryogenic system

Haiyang Ding, Mazen Alamir
Gipsa-lab, CNRS, France
mazen.alamir@grenoble-inp.fr

Francois Bonne
CEA-INAC-SBT, France

Ahmad Hably
Gipsa-lab, Grenoble-INP, France
IEEE member
ahmad.hably@grenoble-inp.fr

Patrick Bonnay
CEA-INAC-SBT, France

***Abstract*—In this paper a recently proposed distributed control framework is applied to the model of a real-life cryogenic plant. The main advantage of the distributed control architecture is to allow for a modular design of the control algorithms. The paper shows that the cooperative nature of the solution enables an initial decentralized design to be improved by properly choosing the relative priority assignment between subsystems.**

I. Introduction

Cryogenic systems are necessary to cool the supra-conducting devices that are used in many physical instruments including nuclear fusion reactors [9], [6] and particle accelerators. Thanks to advances in system modeling in the last decade ([4], [5], [6]), model-based control strategies have been used in order to avoid plants' oversize and to drastically reduce their energy consumption [3], [11], [6], [2]. While the above mentioned works are mainly based on centralized control schemes, the cryogenic system can be viewed as an interconnection of several coupled heterogeneous subsystems with local objectives. The cryogenic practitioners prefer rather modular design framework in which coupling-related issues and solutions are addressed by an additional layer that does not question the old existing widely assessed local controllers. This paper presents the performance of the application of the distributed control framework developed in [1], [8] on a cryogenic system. This is realized by using the model of the experimental helium refrigerator facility located at CEA[1]-INAC[2]-SBT[3], Grenoble, France.

The paper is organized as follows: section II gives an overview of the cryogenic system. The model and the control objectives are presented in section III, while the cooperative distributed framework proposed in [8] is briefly recalled in section IV. The simulation results and analysis are given in section V. Section VI concludes the paper.

II. Overview of the cryogenic system

The cryogenic system located at CEA-INAC-SBT, Grenoble is shown in Fig. 1. This plant offers a nominal capacity of 400 (watts W) at 4.5 (kelvin K) and serves as a testbed on which physical experiments are performed (testing cryogenic components, study of super-fluid helium, etc.) [6]. Fig.2 shows a block diagram of the cryogenic system consisting of a *warm* Compression system and a *cold box* (phase separator) in which the heating device emulates the devices to be cooled. Fig.3 shows the ideal Claude thermodynamic cycle. As illustrated in Fig.2, the Warm Compression System consists of a screw compressor with operational condition between 1.05 bar and 16 bar with a maximum flow rate of 72 $g \cdot s^{-1}$ and three control valves. The operational point of the refrigerator is set by the by-pass valve CV_{956}. It is used to pass the excess flow rate towards the cold box. Control valves CV_{952} and CV_{953} serve respectively to supply or to evacuate the gas from the system via a helium gas drum. The heat load that disturbs the cryogenic system is represented by the resistance NCR_{22} at the bottom of the diagram in Fig.2. The cold box cools down the helium flow from 300 K to 4.5 K using the following equipment:

1) A liquid Nitrogen cooler followed by several counter-flow heat exchangers.
2) A cold turbine expander, controlled by the CV_{156} valve, which extracts work form the gas.
3) A Joule-Thomson expansion valve (CV_{155}).
4) A phase separator with the two-phase helium bath that is connected to the load.

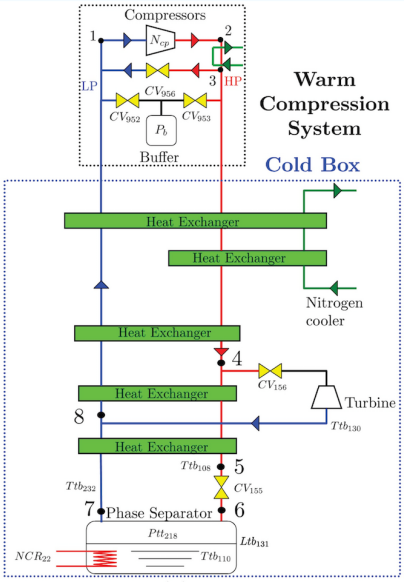

Fig. 2: A block diagram of the cryogenic system consisting of a *warm* compression system and a *cold box* (phase separator) in which the heating device emulates the devices to be cooled

[1]CEA: Commissariat à l'Energie Atomique et aux Energies Alternatives
[2]Institut NAnosciences et Cryogénie
[3]Service des Basses Températures

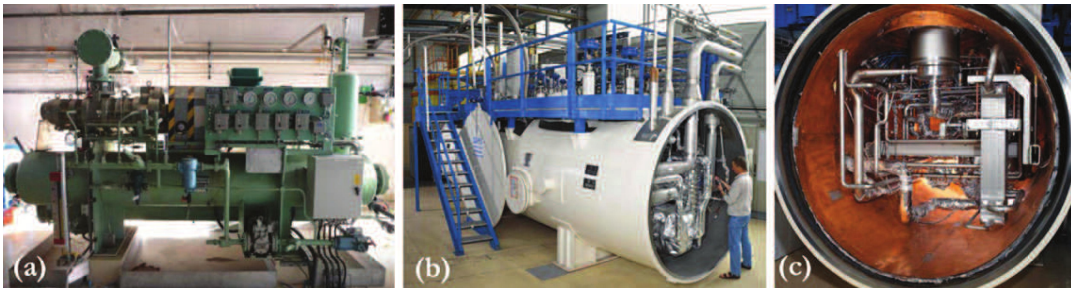

Fig. 1: Photos of the cryogenic plant of CEA-INAC-SBT, Grenoble. (a) The compressor of the warm compression system. (b) Global view of the cold box. (c) Details of the cold box.

III. Model description and control objectives

A. Model description

According to [10], the system can be viewed as the interconnection of four subsystems (see Fig.5): Joule-Thomson cycle (phase separator), Brayton cycle (Turbine), warm end, and warm zone. The cooperative distributed control is applied based on this subdivision of the cryogenic plant and these four subsystems are referred to by $\sum_1$, $\sum_2$, $\sum_3$ and $\sum_4$ in the sequel.

The subsystems are interconnected through their physical outputs listed in Table. I, where the subscripts T, P, M, H and C stand for temperature, pressure, mass of liquid flow, hot and cold respectively. For example, T_{H_4} stands for the output hot temperature of subsystem $\sum_4$.

TABLE I: Outputs of the subsystems of the cryogenic plant

Symbol	Subsystem name	Output
$\sum_1$	phase separator	T_{C_1}, M_{H_1}, M_{C_1}
$\sum_2$	Brayton cycle	T_{H_2}, P_{H_2}, P_{C_2}, T_{C_2}, M_{H_2}, M_{C_2}
$\sum_3$	warm end	T_{H_3}, P_{H_3}, P_{C_3}, T_{C_3}, M_{H_3}, M_{C_3}
$\sum_4$	warm zone	T_{H_4}, P_{H_4}, P_{C_4}

Given the interconnection topology shown in Fig.4, the outputs of subsystems are introduced. Note that $y_{i\to j}$ indicates the output of subsystem $\sum_i$ that affects subsystem $\sum_j$.

$$y_{1\to2} = [T_{C_1}\ M_{H_1}\ M_{C_1}]^T,\ y_{2\to1} = [T_{H_2}\ P_{H_2}\ P_{C_2}]^T$$
$$y_{2\to3} = [T_{C_2}\ M_{H_2}\ M_{C_2}]^T,\ y_{3\to2} = [T_{H_3}\ P_{H_3}\ P_{C_3}]^T$$
$$y_{3\to4} = [T_{C_3}\ M_{H_3}\ M_{C_3}]^T,\ y_{4\to3} = [T_{H_4}\ P_{H_4}\ P_{C_4}]^T$$

The structure of the differential equations governing each subsystem and the corresponding size of the state and control vectors are briefly sketched Below. For an exhaustive presentation including the matrix definitions, the reader can refer to [7]. So one has the following subsystems:

Subsystem $\sum_1$ - Phase separator

$$\dot{\xi}_1 = \overline{A}_1\xi_1 + \begin{bmatrix} \overline{B}_1^u & \overline{B}_1^\nu \end{bmatrix} \begin{bmatrix} u_1 \\ \nu \end{bmatrix} + \overline{B}_{2\to1}y_{2\to1} \quad (1)$$
$$y_{1\to2} = \overline{C}_1\xi_1 + \overline{D}_1 \begin{bmatrix} u_1 \\ \nu \\ y_{2\to1} \end{bmatrix}$$

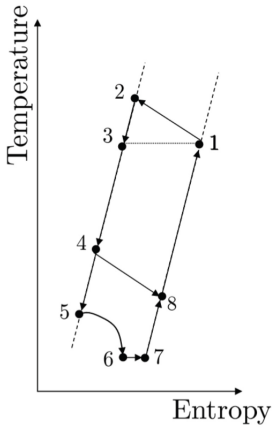

Fig. 3: Ideal Claude thermodynamic cycle

where $\xi_1 \in \mathbb{R}^{17\times1}$ is the state vector of subsystem $\sum_1$, $u_1 \in \mathbb{R}$ is the control input, i.e. the Joule-Thompson expansion valve and ν is the exogenous input (heat load).

Subsystem $\sum_2$ - Brayton cycle/turbine

$$\dot{\xi}_2 = \overline{A}_2\xi_2 + \overline{B}_2^u u_2 + \overline{B}_{3\to2}y_{3\to2} + \overline{B}_{1\to2}y_{1\to2} \quad (2)$$
$$\begin{pmatrix} y_{2\to1} \\ y_{2\to3} \end{pmatrix} = \begin{pmatrix} \overline{C}_{2\to1} \\ \overline{C}_{2\to3} \end{pmatrix} \xi_2 + \overline{D}_2 \begin{bmatrix} u_2 \\ y_{3\to2} \\ y_{1\to2} \end{bmatrix}$$

with $\xi_2 \in \mathbb{R}^{32\times1}$ is the state vector. $u_2 \in \mathbb{R}$ is the control input of subsystem $\sum_2$ i.e. the turbine speed of the Brayton cycle in Fig.5.

Subsystem $\sum_3$ - Warm end

$$\dot{\xi}_3 = \overline{A}_3\xi_3 + \overline{B}_3^u u_3 + \overline{B}_{4\to3}y_{4\to3} + \overline{B}_{2\to3}y_{2\to3} \quad (3)$$
$$\begin{pmatrix} y_{3\to2} \\ y_{3\to4} \end{pmatrix} = \begin{pmatrix} \overline{C}_{3\to2} \\ \overline{C}_{3\to4} \end{pmatrix} \xi_3 + \overline{D}_3 \begin{bmatrix} u_3 \\ y_{4\to3} \\ y_{2\to3} \end{bmatrix}$$

where $\xi_3 \in \mathbb{R}^{50\times1}$ is the state vector and $u_3 \in \mathbb{R}$ is the control input of the Nitrogen cooler shown in Fig.5.

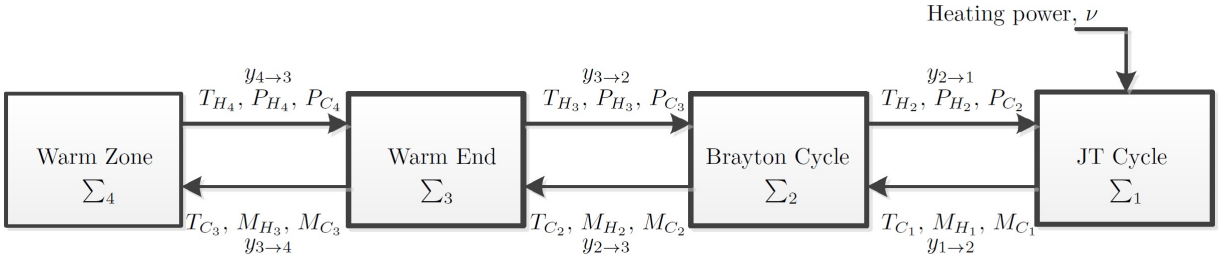

Fig. 4: The interconnection terms between the subsystems of the cryogenic plant.

Subsystem $\sum_4$ - Warm zone

$$\dot{\xi}_4 = \overline{A}_4\xi_4 + \overline{B}_4^u u_4 + \overline{B}_{3\to4}y_{3\to4} \qquad (4)$$
$$y_{4\to3} = \overline{C}_4\xi_4 + \overline{D}_4 \begin{bmatrix} u_4 \\ y_{3\to4} \end{bmatrix}$$

where $\xi_4 \in \mathbb{R}^{2\times1}$ is the state vector and $u_4 \in \mathbb{R}^{2\times1}$ is the control of the warm zone representing the control valves CV_{952} and CV_{953} in Fig.2 which are used to supply or evacuate gas out of the system.

B. Control problem

The main control objective is to maintain the temperature of the liquid helium (T_{helium}) in the phase separator at 4.5 K despite disturbing heat load. Besides this primary task, several constraints regarding security and operational conditions have to be respected, namely:

- The output of the temperature of Brayton cycle $\sum_2$ (T_{H_2} in Fig.4) must remain in the interval $[7.8\text{ K}, 10\text{ K}]$ with set-point $T_{H_2}^{(sp)} = 8.82$ K.
- For security reasons, P_{C_4} of the warm zone and P_{C_2} of the turbine must remain between 1.1 bar and 1.2 bar with set-point $P_{C_4}^{(sp)} = P_{C_2}^{(sp)} = 1.15$ bar.
- The level of liquid helium (H_{level}) in the phase separator (Joule-Thompson cycle) has to stay inside some security interval so that a minimal cooling power is available ($H_{\text{level}} > 20\%$) and not to be overflowed ($H_{\text{level}} < 100\%$) with set-point $H_{\text{level}}^{(sp)} = 50\%$.

The control architecture is defined in a way that each subsystem (with its local control loops) can operate when it is connected or disconnected to the remaining parts. This is particularly true for the compression zone. When the subsystems are interconnected, a cooperation has to take place where each controller's behavior is amended by signals coming only from its neighbors.

IV. The Distributed Control Architecture

In this section, the application of the cooperative distributed control framework [8] to the cryogenic plant is introduced. In order to do this, the dynamic equations (1), (2), (3) and (4) is transformed into the standard form used in [8].

A. Equation transformation

The standard form of the dynamic equations used in the cooperative control framework proposed in [8] is given by:

$$\dot{x}_i = A_i x_i + B_i u_i + \sum_{j\in\mathcal{I}_i^{\leftarrow}} (A_{j\to i}x_j + B_{j\to i}u_j) \qquad (5)$$

A careful examination of equations (1), (2), (3) and (4) shows that they exhibit algebraic loop (for instance $y_{1\to2}$ depends on $y_{2\to1}$ to cite a single example). To eliminate these algebraic loops, a standard state extension technique is used in which additional auxiliary variables are defined that are associated to fast dynamics (1 sec is sufficiently fast for the problem at hand). The extended resulting model becomes:

$$\dot{x}_1 = A_1x_1 + B_1^u u_1 + B_1^\nu \nu + A_{2\to1}x_2 \qquad (6)$$
$$\dot{x}_2 = A_2x_2 + B_2^u u_2 + A_{1\to2}x_1 + A_{3\to2}x_3 \qquad (7)$$
$$\dot{x}_3 = A_3x_3 + B_3^u u_3 + A_{2\to3}x_2 + A_{4\to3}x_4 \qquad (8)$$
$$\dot{x}_4 = A_4x_4 + B_4^u u_4 + A_{3\to4}x_3 \qquad (9)$$

in which u_i, for $i = 1, 2, 3, 4$ and ν keep their meanings in (1)-(4), while $x_i, i = 1, 2, 3, 4$ are the extended states with the following dimensions:

$$x_1 \in \mathbb{R}^{20\times1}, x_2 \in \mathbb{R}^{38\times1}, x_3 \in \mathbb{R}^{56\times1}, x_4 \in \mathbb{R}^{5\times1}$$

The outputs y_i can be expressed in terms of the extended states by $y_i = \bar{C}_i x_i$ (see [7] for a complete description).

B. Control design

1) **Local control design:** The local controller of each subsystem is designed at its nominal point as if it was alone, that is to say, using the following nominal equation:

$$\dot{x}_i = A_i x_i + B_i^u u_i$$

The closed-loop feedback gain K_i for subsystem $\sum_i$ is calculated by LQR design minimizing the cost function:

$$J = \int_0^\infty x_i^T(\tau)Q_i x_i(\tau) + u_i^T(\tau)R_i u_i(\tau)d\tau$$

with $Q_i = p_i \cdot \mathbb{I} + q_i \cdot \overline{C}_i^T\overline{C}_i$, $R_i = r_i \cdot \mathbb{I}$[4]. The values of the parameters used in the nominal LQR design are given in Table.II[5].

[4] $\mathbb{I}$ stands for the identity matrix with a suitable dimension

[5] See the appendix for the definitions of $\hat{C}_i$

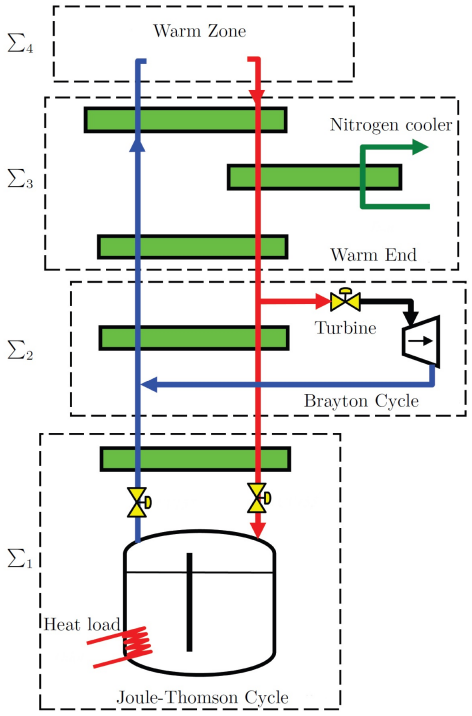

Fig. 5: A schematic view of the cryogenic system in which the plant is viewed as the interconnection of 4 subsystems.

TABLE II: Values of the parameters used in the nominal LQR design

Subsystem	p_i	q_i	r_i	$\overline{C}_i$
$\sum_1$	1	10^3	1	s.t. $T_{helium} = \overline{C}_1 x_1$
$\sum_2$	0	1	10^{-2}	$\overline{C}_2 = \hat{C}_2$
$\sum_3$	0	1	10^{-2}	$\overline{C}_3 = \hat{C}_3$
$\sum_4$	0	1	10^2	$\overline{C}_4 = \hat{C}_4$

The design is intentionally simple in order to show that the cooperative scheme is capable to recovery even with *loosely* locally designed loops. The resulting closed-loop feedback gain for nominal control is K_i for subsystem $\sum_i$. Thus the control of subsystem $\sum_i$ can be written as:

$$u_i = -K_i x_i + v_i \tag{10}$$

in which v_i is the cooperative control term that is to be determined by the cooperative control algorithm.

2) **Cooperative control design:** The cooperative control proposed in [8] involves the definition of priority coefficients π_j^i that describes how important subsystem j is viewed by subsystem i. Given the "chain-like" graph corresponding to the coupling expressed by (6)-(9), the corresponding priority matrix takes the following form:

$$\Pi = \begin{bmatrix} \pi_1^1 & \pi_2^1 & 0 & 0 \\ \pi_1^2 & \pi_2^2 & \pi_3^2 & 0 \\ 0 & \pi_2^3 & \pi_3^3 & \pi_4^3 \\ 0 & 0 & \pi_3^4 & \pi_4^4 \end{bmatrix} \quad ; \quad \pi_i^j \geq 0 \tag{11}$$

Recall that in the cooperative framework of [8], when $\sum_i$ is affected by $\sum_j$, the following quantity is sent by $\sum_i$ to $\sum_j$

$$W_{i \rightarrowtail j} := L^{j \rightarrow i}(x_i) = 2{x_i}^T P_i \tag{12}$$

in which P_i is the corresponding solution to the Riccati equation when defining the LQR control of subsystem $\sum_i$. This information is crucial if $\sum_j$ is willing to cooperate with $\sum_i$ because $W_{i \rightarrowtail j} A_{j \rightarrow i} x_j$ represents the additional term in the derivative of the Lyapunov function $x_i^T P_i x_i$ of $\sum_i$ that comes from the interaction with $\sum_j$. By doing so, $\sum_j$ can incorporate all such terms coming from its neighbors in order to define a cooperative optimal control problem according to:

$$\min_{v_j} \left\{ \|v_j\|_{R_j}^2 + \sum_{i \in \mathcal{I}_j^{\rightarrow}} \pi_j^i W_{i \rightarrowtail j} A_{j \rightarrow i} x_j \right\} \tag{13}$$

It is then shown in [8] that by defining the extended state z_j which gathers x_j and all the terms $\{\pi_j^i W_{i \rightarrowtail j}\}_{i \in \mathcal{I}_j^{\rightarrow}}$ coming from all the subsystems i that are affected by $\sum_j$ (this is denoted by $i \in \mathcal{I}_j^{\rightarrow}$), the cooperative optimal control problem viewed by $\sum_j$ can be put in the following form (see [8] for the detailed expressions):

$$\dot{z}_i = \mathcal{A}_i z_i + \mathcal{B}_i v_i \tag{14}$$

while the cost function (13) rewritten in terms of the extended states z_i in (14) becomes:

$$\min_{v_i} \left\{ {v_i}^T R_i v_j + {z_i}^T Q_i^{coop} z_i \right\} \tag{15}$$

for an appropriate definition of Q_i^{coop} see [8]. By solving the quadratic problem (15), the discrete-time cooperative control term $v_i(k) = K_i^v z_i(k)$ can be obtained and injected in (10). Note also that as far as linear networks of systems are concerned, [8] proposes a systematic procedure for priority assignment that guarantees the stability of the whole system under the cooperative control framework described above.

V. Simulations

Recall that the control objective is to reject heating disturbances that are applied in the bath in order to emulate the heat pulses coming from the supra-conducting devices. Fig. 6 shows the profile of the heating power injected to subsystem $\sum_1$ in all the simulations illustrated in this section. A similar heating power profile has been used in [6]. Besides the outputs of the subsystems, the evolution of nominal Lyapunov functions are also used to evaluate the performance

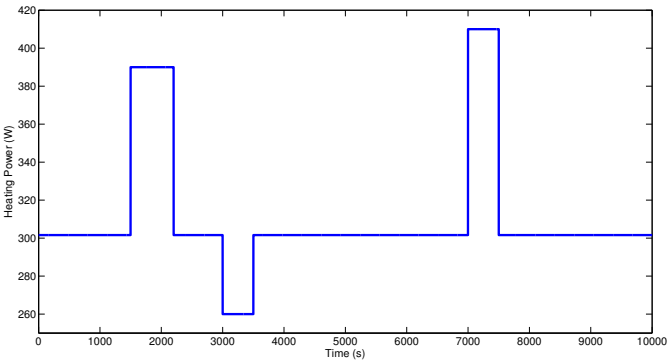

Fig. 6: Heating power profile injected into the cryogenic system.

of the cooperative distributed control. The nominal Lyapunov function of subsystem $\sum_i$ is defined as:

$$\overline{V}_i = {x_i}^T P_i x_i \tag{16}$$

in which P_i is the solution to the corresponding Riccati equation when designing the nominal LQR regulator for subsystem $\sum_i$. Note that when the subsystem is at its operational point, the value of the nominal Lyapunov function is zero.

Due to the fact that the four subsystems of the cryogenic plant are different, the comparison shown hereafter focuses on the so called normalized nominal Lyapunov functions (N-N Lyapunov function) that is defined by:

$$V_i^{s_1} = \frac{\overline{V}_i^{s_1}}{V_i^{max}}, \quad V_i^{s_2} = \frac{\overline{V}_i^{s_2}}{V_i^{max}}$$

where s_1 and s_2 denote two different assignments of control framework parameters explained later, while V_i^{max} is the maximum value of the two nominal Lyapunov functions along their evolution for subsystem $\sum_i$ in each set of comparison between the priority settings denoted by s_1 and s_2, namely:

$$V_i^{max} = \max_{k\in\{1,\cdots,N_s\}} \left\{ \max\left\{\overline{V}_i^{s_1}(k)\right\}, \max\left\{\overline{V}_i^{s_2}(k)\right\} \right\}$$

where N_s is the simulation length. In some simulations, the performances are compared by referring to the residual of the N-N Lyapunov functions defined by:

$$\Delta V_i = V_i^{s_1} - V_i^{s_2} \tag{17}$$

Note that when ΔV_i is negative, then assignment s_1 is better than s_2 as far as the subsystem i is concerned.

The behavior of the cryogenic system under the decentralized control-loop (i.e. the cooperative control is deactivated by using $v_i = 0$ for all i, denoted by "non-cooperative control") is compared with the distributed control with equal priority assignment Π_{equal} (i.e π_i^j in (11) equals 1) and then with distributed cooperative control with high priority given to the warm compression subsystem Σ_4 (i.e. the priority matrix Π_4 is chosen with $\pi_4^j = 2$ (for $j = 3, 4$)). The results are shown in Fig.7, the N-N Lyapunov function of cooperative control (V_i^{coop}) is systematically less than that of non-cooperative control ($V_i^{noncoop}$).

The outputs of subsystems are illustrated in Figs. 8-10. One can clearly notice that P_{C_4} violates its constraints ($P_{C_4} \leq 1.2$ bar) (Fig.8) in non-cooperative control while this constraint is fulfilled under cooperative control. By giving high priority to the warm zone ($\sum_4$) by Π_4, the performances of all subsystems are improved when compared to the equal priority setting. So it can be concluded that the priority assignment Π_4 which emphasizes the importance of the warm zone allows improved effectiveness of the cooperative control framework.

VI. Conclusion

In this paper, the cooperative control proposed in [8] is applied to a cryogenic plant which can be viewed as the interconnection of four subsystems with individual tasks. Comparing to the non-cooperative control strategy in which only nominal controller is activated, the cooperative control with equal priority improves the performance of the cryogenic plant under non-modeled disturbance (heating power) at the phase separator. Moreover, it is found that by assigning high priority to the warm zone, the effectiveness of the cooperative control framework is further improved.

Future work is currently in progress thanks to the French ANR-Cryogreen project in which nonlinear constrained local controllers are expected to be used. The objective of this extension is twofold: perform an explicit constraints handling and fully exploit the knowledge-based models that are sometimes nonlinear while avoiding the contamination of these nonlinearities on the overall system. This can be achieved by replacing the controlled nonlinear subsystems (under their nonlinear feedback) by appropriate resulting nonlinear model with the right response time and use the resulting linear models to assign the priority coefficient following the algorithms proposed in [8].

Acknowledgment. The authors are grateful to the financial support from the National French Research Agency (ANR) through the CRYOGREEN project but also through the former CHEOPS project.

Appendix

The details on equation transformation to eliminate the algebraic loops from the cryogenic plant are given in [8]. In this section only the definitions of the $\hat{C}_i$ are given:

$$\begin{aligned}
\hat{C}_1 &= [\bar{C}_{1\to 2} \quad \mathbb{I}_{3\times 3}] \\
\hat{C}_2 &= \begin{bmatrix} \bar{C}_{2\to 1} & \mathbb{I}_{3\times 3} & \mathbb{O}_{3\times 3} \\ \bar{C}_{2\to 3} & \mathbb{O}_{3\times 3} & \mathbb{I}_{3\times 3} \end{bmatrix} \\
\hat{C}_3 &= \begin{bmatrix} \bar{C}_{3\to 2} & \mathbb{I}_{3\times 3} & \mathbb{O}_{3\times 3} \\ \bar{C}_{3\to 4} & \mathbb{O}_{3\times 3} & \mathbb{I}_{3\times 3} \end{bmatrix} \\
\hat{C}_4 &= [\bar{C}_{4\to 3} \quad \mathbb{I}_{3\times 3}]
\end{aligned}$$

Note that the notation $\mathbb{O}_{a\times b}$ and $\mathbb{I}_{a\times b}$ represent respectively the zero matrix and the identity matrix of size $(a \times b)$.

REFERENCES

[1] M. Alamir, A. Hably, and H. Ding. A novel distributed nmpc control structure for partially cooperative systems under limited information sharing. In *Proceedings of the 18th IFAC World Congress*, 2011.

[2] F. Bonne, M. Alamir, and P. Bonnay. Nonlinear observers of the thermal loads applied to the helium bath of a cryogenic joule-thompson cycle. *Journal of Process Control*, 24(3), 2014.

[3] B. Bradu, Ph. Gayet, and S.I. Niculescu. Control optimization of a lhc 18kw cryoplant warm compression station using dynamic simulations. In *AIP conference proceedings*, 2010.

[4] Benjamin Bradu, Philippe Gayet, and Silviu-Iulian Niculescu. Modeling, simulation and control of large scale cryogenic systems. In *Proceedings of the 17th World Congress The International Federation of Automatic Control*, 2008.

[5] Benjamin Bradu, Philippe Gayeta, and Silviu-Iulian Niculescub. A process and control simulator for large scale cryogenic plants. *Control Engineering Practice*, 17:1388–1397, 2009.

[6] F. Clavel, M. Alamir, P. Bonnay, A. Barraud, G. Bornard, and C. Deschildre. Multivariable control architecture for a cryogenic test facility under high pulsed loads: Model derivation, control design and experimental validation. *Journal of Process Control*, 21:1030–1039, 2011.

[7] H. Ding. *On a partially cooperative distributed control framework with priority assignement*. PhD thesis, University of Grenoble, 2013.

[8] H. Ding, M. Alamir, and A. Hably. A distributed cooperative control scheme with optimal priority assignment and stability assessment. In *Proceedings of the 19th IFAC World Congress*, 2014.

[9] D. Henry, J. Y. Journeaux, P. Roussel, F. Michel, J. M. Poncet, A. Girard, V. Kalinin, and P. Chesny. Analysis of the iter cryoplant operational modes. *Fusion Engineering and Design*, 82:1454–1459, 2007.

[10] Pawel Majecki. Control-oriented modelling of the cold boc of the cryogenic station 400w@4.5k. Technical report, INAC, Direction des Sciences et de la Matire, Institut naosciences ey Cryognie, Service des Basses Temperattures, 2011.

[11] E. Blanco Vinuela, J. Casas Cubillos, and C. de Prada Moraga. Linear model-based predictive control of the lhc 1.8k cryogenic loop. In *Cryogenic Engineering and International Cryogenic Materials Conference*, 1999.

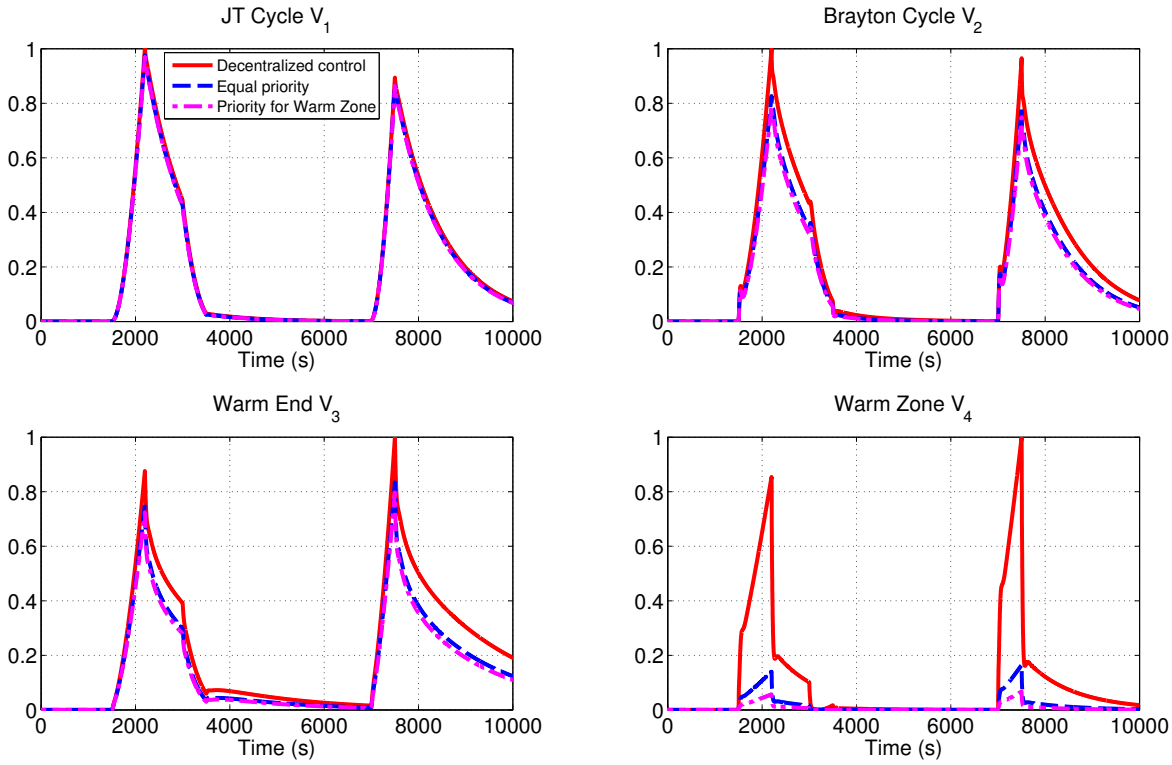

Fig. 7: Evolution of the N-N Lyapunov functions of the subsystems under non-cooperative control (solid red), cooperative control with equal priority (dashed blue), and cooperative control with priority for warm zone. In general, the N-N Lyapunov function of cooperative control is less than that of the non-cooperative control.

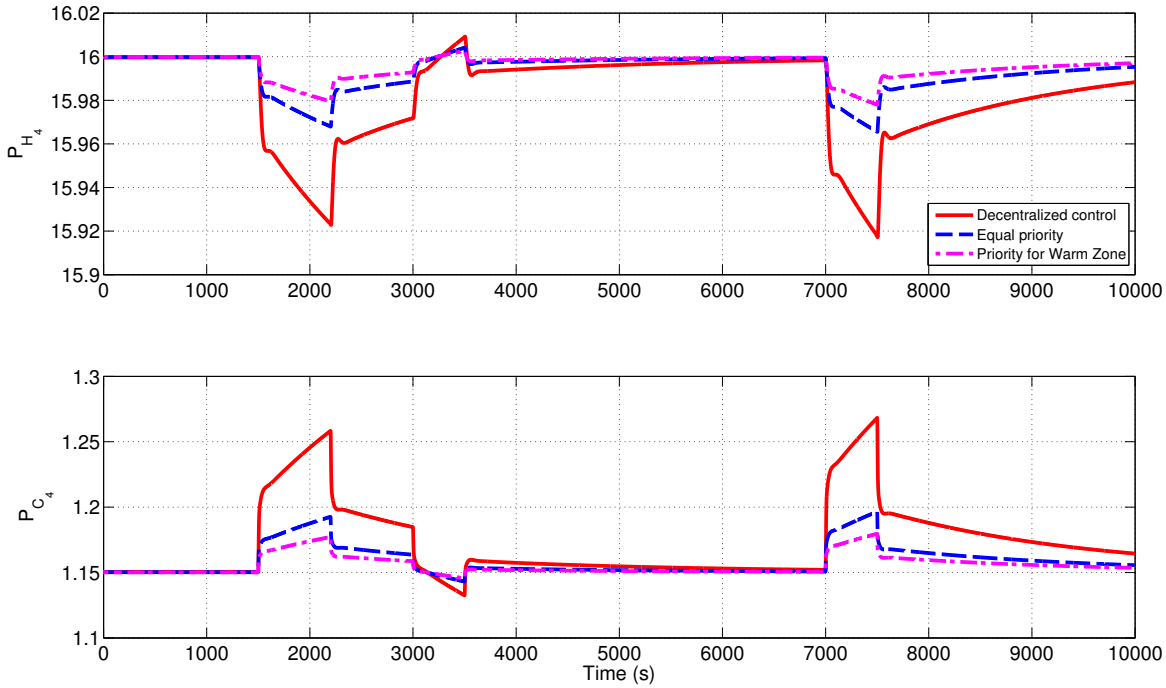

Fig. 8: P_{C_4} and P_{H_4} under decentralized control (solid red) cooperative control with equal priority (dashed blue) and cooperative control with priority for the warm zone (violet). In the non-cooperative control, P_{C_4} goes beyond its upper limit (1.2 bar). In addition, the performance is improved with cooperative control. When the warm zone is given a high priority P_{C_4} and P_{H_4} are better regulated by cooperative control.

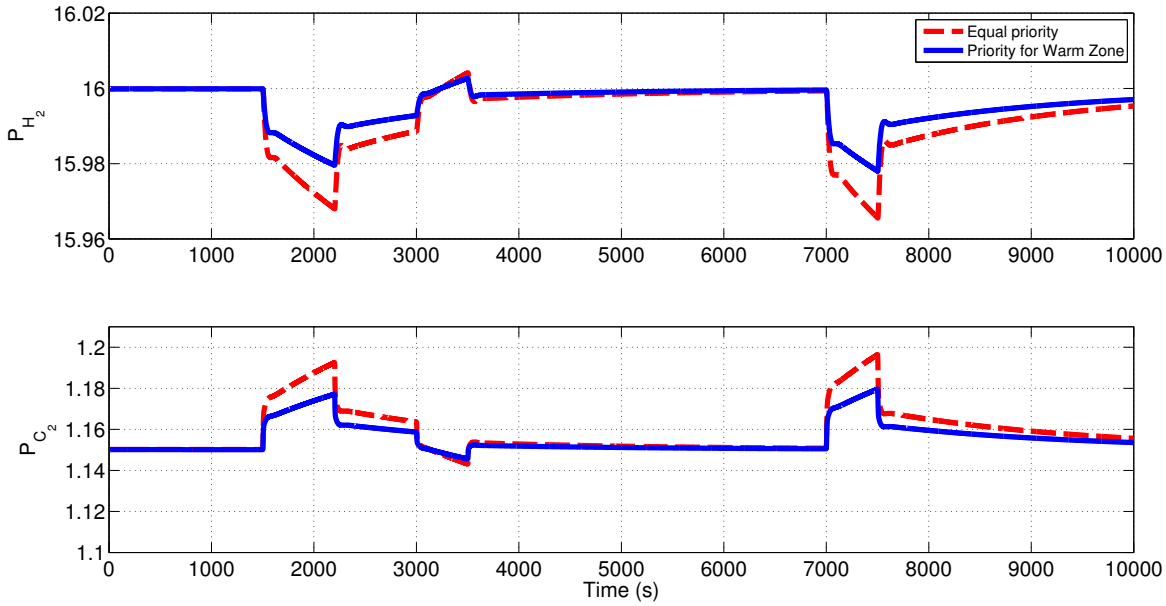

Fig. 9: P_{C_2} and P_{H_2} achieve improved performances although high priority is assigned to the warm zone.

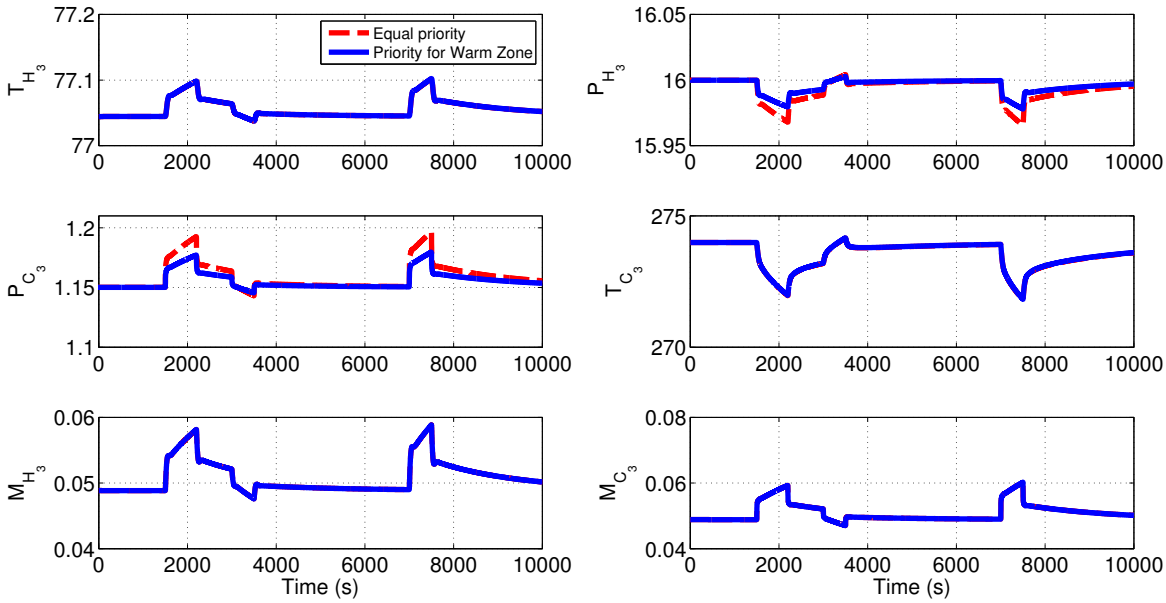

Fig. 10: The outputs of subsystem $\sum_3$ with high priority to the warm zone.